Applied Energy 183 (2016) 504–512

Contents lists available at ScienceDirect

Applied Energy

journal homepage: www.elsevier.com/locate/apenergy

Quantifying impacts of heat waves on power grid operation ☆

Xinda Ke [b], Di Wu [b,*], Jennie Rice [b], Michael Kintner-Meyer [b], Ning Lu [a]

[a] North Carolina State University, Raleigh, NC 27606, USA
[b] Pacific Northwest National Laboratory, Richland, WA 99354, USA

HIGHLIGHTS

- Heat waves cannot only increase the electricity load, but also derate gas turbines.
- Derating in capacity and efficiency is characterized as functions of ambient temperature.
- The derating models are integrated into a modified MILP unit commitment formulation.
- The production cost model is coupled with hourly temperature data and load model.
- Heat wave impacts on grid are quantified from reliability and economics perspectives.

ARTICLE INFO

Article history:
Received 22 March 2016
Received in revised form 29 August 2016
Accepted 30 August 2016
Available online 10 September 2016

Keywords:
Climate change
Heat wave
Power grid operation
Production cost model
Unit commitment

ABSTRACT

Climate change is projected to cause an increase in the severity and frequency of extreme weather events such as heat waves and droughts. Such changes present planning and operating challenges and risks to many economic sectors. In the electricity sector, statistics of extreme events in the past have been used to help plan for future peak loads, determine associated infrastructure requirements, and evaluate operational risks, but industry-standard planning tools have yet to be coupled with or informed by temperature models to explore the impacts of the "new normal" on planning studies. For example, high ambient temperatures during heat waves reduce the output capacity and efficiency of gas-fired combustion turbines just when they are needed most to meet peak demands. This paper describes the development and application of a production cost and unit commitment model coupled to high resolution, hourly temperature data and a temperature-dependent load model. The coupled system has the ability to represent the impacts of hourly temperature on load conditions and available capacity and efficiency of combustion turbines, and therefore capture the potential impacts on system reserve and production cost. Ongoing work expands this capability to address the impacts of water availability and temperature on power grid operation.

1. Introduction

Since the start of 20th century, the average annual temperatures across United States have increased approximately 0.8 °C, with 2001–2010 being the warmest decade ever recorded [1]. Global warming not only causes average temperature to rise but also leads to more frequent and severe extreme weather events such as heat waves [2] and droughts [3]. Quantifying the impacts of those extreme weather events on the reliability and operation of the power grid is becoming increasingly important, especially when large amounts of renewable resources and gas turbines have displaced coal power plants, which are less susceptible to variation of temperature, precipitation, and wind.

During the past few years, many research efforts have been dedicated to study the impacts of climate change on electric power grids from different aspects. In [4], the benefits of power transfers between the Pacific Northwest and California were evaluated using a linked set of hydrologic, reservoir, and power demand simulation models for the Columbia River and the Sacramento-San Joaquin reservoir systems. In [5], Cohen et al. investigated the potential impacts of water availability in generation capacity expansion planning using Regional Energy Deployment System (ReEDS) and compared electricity sector growth with and without climate-influenced water rights. In [6], the impacts of temperature change

☆ This material is based upon work supported by the U.S. Department of Energy, Office of Science, Office of Biological and Environmental Research as part of the Integrated Assessment Research Program. The Pacific Northwest National Laboratory is operated for DOE by Battelle Memorial Institute under contract DE-AC05-76RL01830.

* Corresponding author.
E-mail address: di.wu@pnnl.gov (D. Wu).

http://dx.doi.org/10.1016/j.apenergy.2016.08.188
0306-2619/

Nomenclature

Constants

B_g	fuel price of unit g
C_g^{fix}	fixed (no-load) cost of unit g
C_g^{up}, C_g^{dn}	startup and shutdown cost of unit g
$F_l(t)$	maximum power flow of path l in period t
G	number of generation units in the system
$H_{g,n}$	heat rate of block n of the piecewise linear cost function of unit g in period t
$L_i(t)$	load in zone i in period t
N_g	number of blocks of the piecewise linear cost function of unit g
$P_g^{\min}$, $P_g^{\max}$	minimum and maximum power output of unit g
$P_{g,n}$	maximum power that can be produced in block n of the piecewise linear cost function of unit g
R_g^{up}, R_g^{dn}	ramp up and down rate of unit g
$R_i(t)$	system reserve requirement of zone i in period t
T	length of the planning horizon
T_g^{up}, T_g^{dn}	minimum up and down time of unit g, which are expressed as integer number of periods
$\eta_g^{\text{cap}}(t)$	capacity derating of unit g in percentage of the maximum power output in period t
$\eta_g^{\text{eff}}(t)$	efficiency derating of unit g in percentage of the heat rate in period t
ΔT	duration of each period

Variables

$c_g(t)$	production cost of unit g in period t
$f_l(t)$	power flow of path l in period t
$p_g(t)$	total power output of unit g in period t
$p_{g,n}(t)$	power output in block n of the piecewise linear cost function of unit g in period t
$r_g(t)$	reserve provided by unit g in period t
$u_g(t)$	binary variable that equals to 1 if unit g is online in period t and 0 otherwise
$x_g(t)$	transition (startup or shutdown) cost of unit g in period t

on electricity demand were quantified by combining the simulation of climate with building end uses. Zhou et al. projected state-level buildings energy demand and its spatial pattern through the end of the century, considering the impact of climate change based on the estimates of heating and cooling degree days derived from downscaled USGS CASCaDE temperature data [7]. To quantify hourly temperature-dependent building energy demands, Dirks et al. developed the Building ENergy Demand (BEND) model, which is based on detailed thermal dynamic simulation [8]. In [9], Kraucunas et al. developed an innovative modeling system called the Platform for Regional Integrated Modeling and Analysis to simulate interactions among natural and human systems at scales relevant to regional decision making. Various climate change mitigation strategies related to the power grid have also been investigated. For example, Wang et al. reviewed smart grids and renewable energy technologies recently developed to mitigate the impacts of power systems on climate change [10]. In [11], Cohen et al. proposed a versatile optimization model that maximizes profits at a fossil-based power plant with CO_2 capture to better understand performance and economics of CO_2 capture technology. Wu and Aliprantis evaluated the potential reduction in greenhouse gas emissions from energy and transportation systems using plug-in electric vehicle technology in [12]. de la Rue du Can et al. proposed a method to allocate carbon dioxide emissions to the end-use sectors to improve the understanding of emission reduction actions for mitigation of climate change in [13]. In this paper, we focus on quantifying the impacts of heat waves on power grid operation.

Heat waves could have significant impacts on power system operation, such as increased peak loads and reduced transmission and generation capacity, as conceptually illustrated in Fig. 1. When a heat wave comes, the hot weather can last from days to weeks. Because more than 60% of the load is for cooling needs in summer, power system peak loads can be much higher than usual in both magnitude and duration [14]. Higher ambient temperatures also reduce thermal capacity of transmission lines, which further stresses the power grid. Heat waves are usually accompanied by stationary high pressure zones, resulting in light winds at the surface and therefore reduced wind generation. Moreover, increased air temperature also causes derating effects, i.e., reduced capacity and efficiency of gas-turbine (GT) and combine-cycle gas

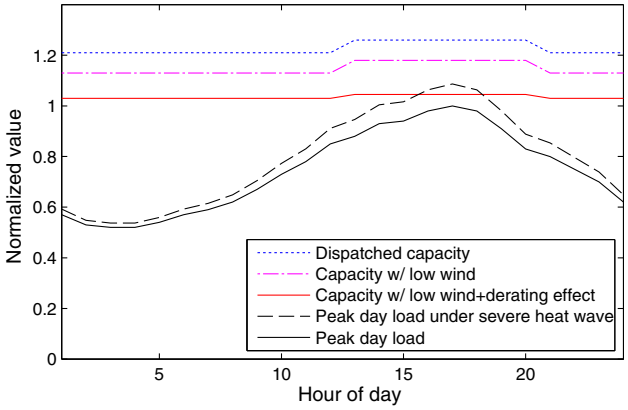

Fig. 1. Illustration of impacts of heat waves on power system operation.

turbines (CCGT) [15–17]. Such a deficiency in supply could result in severe problems in power system operation.

Production cost tools are used extensively in the electric power industry to estimate the expected cost of supplying the system load while providing operation reserves for meeting system reliability requirements. Existing regional level studies are normally conducted using commercial production cost tools such as PROMOD [18] and PLEXOS [19], which rely on hourly chronological simulation of unit commitment (UC). Literature review shows that although formulation and solution techniques of UC problems have been well researched in the past [20–24], the coupling between UC in production cost model and temperature-dependent models has not been adequately considered. In [25], Valenzuela et al. researched the influence of uncertainty in temperature forecast on short-term system operational cost using stochastic methods. In [26], Geng et al. proposed a mixed integer quadratic programming formulation to incorporate the weather-responsive characteristics of CCGT in UC formulation. As previously explained, high temperature during heat waves affects both system load and generation units. Without modeling and capturing effects on both sides, one cannot quantify the overall impacts of heat waves on grid operation. This paper describes the development and applica-

tion of a production cost model for quantifying impacts of heat waves on power grid operation considering both temperature-dependent load and generators (GT and CCGT). In the proposed method, we explicitly incorporate a generator derating model into UC formulation in the production cost model, which is then coupled with high spatial and temporal resolution of temperature data and the temperature-dependent load model, so that hourly or intra-hour system impacts can be captured. The main technical challenge of considering the derating effects is that output capacity and net efficiency of GT and CCGT will vary on an hourly basis. In this paper, hourly derating impacts is reflected through a modified mixed integer linear programming (MILP) UC formulation, which is different from [25,26]. Another feature that differentiates this paper from previous studies is that heat wave impacts are quantified from the viewpoints of production cost and system reserve. Furthermore, small IEEE test systems with very a few generators were used in previous studies such as [25,26] to demonstrate and validate the proposed method and formulation. Practical power systems are needed to provide more meaningful analytical results to power system researchers and practitioners. Because the numbers of GT and CCGT are significant in a practical large grid, such as the Eastern Interconnection (EIC), this temperature dependency requires significant data preprocessing of spatially and temporally distributed data to modify the hourly changing constraints and cost functions in the UC problem. This paper will discuss how hourly temperature profiles affect the UC formulation and production cost analysis. As will be shown, the heat wave impacts can be addressed without increasing the dimension of the UC problem. The main contributions of this paper are twofold. First, we model the derating impacts on GT and CCGT and modify MILP UC formulation to incorporate the derating model. Second, we implement the modified UC formulation and compare the results with existing production cost analysis methods.

The rest of this paper is organized as follows. In Section 2, hourly derating effects on GT and CCGT plants are characterized and incorporated into UC problem formulation. Different scenarios are studied using the EIC system in Section 3 to demonstrate and quantify derating impacts from the viewpoints of production cost and system reserve. Section 4 presents concluding remarks.

2. Methodology

GT and CCGT are less pollutant, more efficient, and less costly compared with conventional coal plants [27]. They are the most important two types of gas-fired plants in the power generation fleet in the U.S., combined together accounting for 27.4% of the nation's annual electricity generation [28]. This number is expected to increase in the future [29], making the derating effects even more severe for reliable and economic operation of power systems during heat waves. This section will first characterize the derating of GT and CCGT units as functions of ambient temperature. The derating model is then incorporated into the UC formulation in production cost analysis.

2.1. Characterization of temperature impacts on combustion turbine

A combustion turbine is a dynamic internal combustion engine that has a compressor coupled with a downstream turbine through a combustion chamber. Its power output capacity and efficiency depend on the ambient temperature because any change in ambient temperature will affect inlet air flow mass, and consequently the power produced from a gas turbine. For a large power system, ambient temperature can vary dramatically at different geographic locations in different seasons. Taking EIC as an example, temperature in Texas frequently exceeds 35 °C in summer, while in Ontario, Canada, temperature can sometimes drop below −30 °C in winter. In addition, the variation of temperature within a day could also be large, especially during heat waves. As an example, the temperature during a historical heat wave in Houston in 2000 is plotted together with the average value from 2000 to 2012 for a few days between August and September in Fig. 2. As can be seen, during this heat wave, the highest temperature is 43 °C and the lowest is 23 °C. As results, the actual output capacity and efficiency of combustion turbines can vary significantly between day and night.

2.1.1. Capacity derating

Capacity derating is typically modeled on a monthly basis in commercial software packages, as illustrated in Fig. 3. The generation capacity generally increases in winter months when temperature is low and decreases in summer months when temperature is high. Such adjustment is able to capture seasonal variation in temperature and in generation capacity. Nevertheless, the variation of actual capacity within a day can also be large, especially during heat waves. Because surging temperature usually corresponds to peak electric power demand, the reduction in generation capacity during heat waves is normally more problematic. To better capture this variation in capacity, we need to express the capacity derating as a function of ambient temperature, and then adjust capacity according to ambient temperature with increased temporal resolution.

The air mass contained in per unit volume decreases with increasing temperature. Less air mass results in less fuel mass that can be ignited, and therefore reduced power output. Based on GT data sheets in [30], the relationship between capacity derating rate α (unitless) and ambient temperature θ (in Celsius) for GT can be expressed as

$$\eta = \begin{cases} (-0.6854\theta + 110)/100, & \theta \geqslant 0, \\ 1.10, & \theta < 0. \end{cases} \quad (1)$$

Operation of the combustion mode is assumed to account for 50% of power output from a CCGT. Therefore, its capacity derating rate is half of GT. The derating rates for GT and CCGT as a function of ambient temperature are plotted in Fig. 4. With such derating functions, we are able to couple the capacity of each GT/CCGT unit in UC formulation with hourly temperature data.

2.1.2. Efficiency derating

Heat rate is a term commonly used in power systems to indicate the power plant efficiency. It is defined as the amount of energy used by a generator to produce one unit of electricity output. The heat rate is the inverse of efficiency—a lower heat rate is better. The combustion gas turbine burns an air-fuel mixture in combustion chamber to produce hot vapor for spinning the turbine.

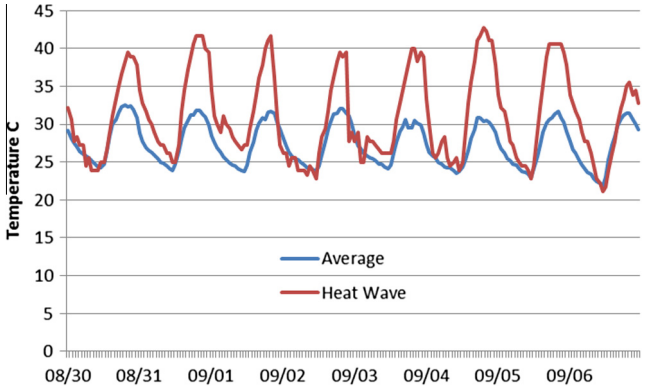

Fig. 2. Temperature during a heat wave in 2000 vs. average value in Houston.

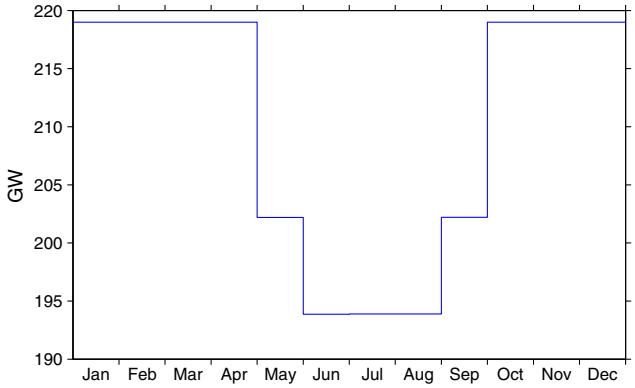

Fig. 3. Monthly total capacity from GT and CCGT in EIC in 2006.

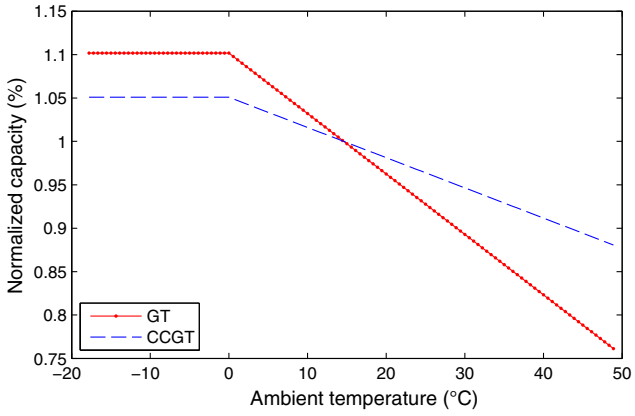

Fig. 4. Normalized capacity as a function of ambient temperature.

However, the density of input air decreases with increasing ambient temperature, resulting in more fuel needed to compress the same amount of air mass. The increased fuel consumption per unit energy output leads to increased heat rate and decreased net efficiency of a GT/CCGT unit [31], which is typically not modeled in commercial software packages. The normalized heat rate can be expressed as a function of ambient temperature, as shown in Fig. 5. Using such derating functions combined with hourly temperature data, we are able to adjust fuel efficiency on an hourly basis in the UC formulation in production cost model.

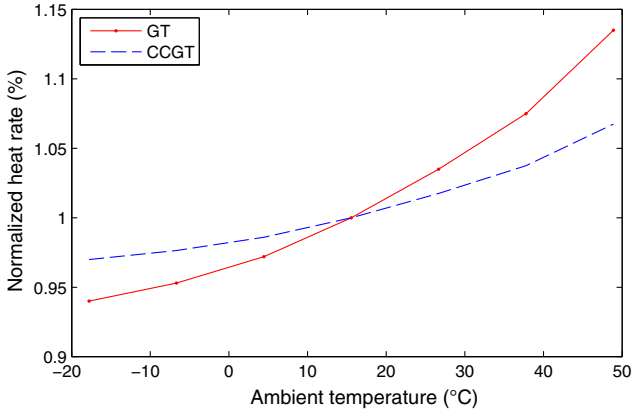

Fig. 5. Normalized heat rate as a function of ambient temperature.

2.2. Incorporation of derating model in UC formulation

The UC problem seeks to find the lowest cost schedule to commit/uncommit a fleet of units over an operational planning horizon to meet the demand, while adhering to system and individual generator constraints. The formulation of UC as a MILP problem can be found in many existing publications such as [20,22,32]. With hourly varying ambient temperature, the output capacity and heat rate of GT and CCGT units need to be adjusted. This will affect both the objective function and some constraints in the UC problem. For readers' convenience, we herein present the entire UC formulation including the equations that are not affected by ambient temperature.

2.2.1. Objective function

The objective of UC problem is to minimize the total operation cost, which is the sum of the production cost and transition cost over the UC time span T, as expressed in (2).

$$\min \sum_{t=1}^{T}\sum_{g=1}^{G}\left(c_g(t)+x_g(t)\right) \tag{2}$$

where $c_g(t)$ represents production cost of unit g in period t, and $x_g(t)$ represents transition cost unit g in period t.

- The production cost is typically expressed as a quadratic function of the power output [33]. In MILP formulation of UC problem, this quadratic production cost function is typically approximated by a linear representation, including fixed cost and a set of piecewise blocks of variable cost [20], as expressed in (3).

$$c_g(t) = C_g^{\text{fix}}u_g(t) + B_g\sum_{n=1}^{N_g}p_{g,n}(t)\Delta T\frac{H_{g,n}}{\eta_g^{\text{eff}}(t)} \tag{3}$$

where $u_g(t)$ is the on/off status of unit g in period t, C_g^{fix} is the fixed (no-load) cost of unit g, B_g is the fuel price of unit g, N_g is the number of blocks of the piecewise linear cost function of unit g, ΔT is the time step size, $H_{g,n}$ is the nominal heat rate of unit g in block n, $\eta_g^{\text{eff}}(t)$ is efficiency derating of unit g in percentage of the heat rate in period t, and $p_{g,n}(t)$ is the power output in block n of the piecewise linear cost function of unit g in period t, which must satisfy

$$0 \leqslant p_{g,n}(t) \leqslant P_{g,n}u_g(t), \tag{4}$$

where $P_{g,n}$ denotes the maximum power that can be produced in block n of the piecewise linear cost function of unit g. In (3), it is $\eta_g^{\text{eff}}(t)$ that captures the derating effect in heat rate during heat waves and therefore, the impacts on system operation cost. Moreover, high temperature during heat waves also causes capacity derating, which ultimately affects the power output $p_{g,n}(t)$ in some piecewise blocks. Nevertheless, such impacts are captured through derating the maximum generation output of generators, as will be described in generator unit constraints later.

- Transition cost includes startup and shutdown cost. Startup cost involves both fixed cost and variable cost. Variable cost is typically a function of off-line time and can be approximated by step functions [34]. Shutdown cost generally involves only fixed cost (mainly labor) and is relatively easy to model. Because heat waves and generator derating do not affect the transition cost formulation, herein we present a simplified version of the startup cost function with only one step. The transition cost in (2) must satisfy (5)

$$x_g(t) \geqslant C_g^{up}\big(u_g(t) - u_g(t-1)\big), \tag{5a}$$

$$x_g(t) \geqslant C_g^{dn}\big(u_g(t-1) - u_g(t)\big), \tag{5b}$$

$$x_g(t) \geqslant 0, \tag{5c}$$

where C_g^{up} and C_g^{dn}, respectively, represents the startup and shutdown cost of unit g.

2.2.2. Constraints

UC formulation includes both unit and system constraints, which are described as follows.

- Unit constraints considered in this paper include power output limits, minimum up/down time, and ramp rate. The power output of each unit is capped by its minimum and maximum power limits,

$$P_g^{min} \leqslant p_g(t) \leqslant \eta_g^{cap}(t) P_g^{max}, \tag{6}$$

where P_g^{min} is the minimum output, P_g^{max} is the nominal capacity of unit g, $p_g(t)$ is the total power output of unit g in period t, which is equal to $\sum_{n=1}^{N_g} p_{g,n}(t)$, and $\eta_g^{cap}(t)$ represents capacity derating factor of generator g in period t, which reflects the reduction in capacity caused by increasing temperature. Because thermal units can undergo only gradual temperature changes, units that are committed must remain committed for a minimum amount of time. Likewise, units that are de-committed must remain down for a minimum amount of time. Minimum up/down time limits are ensured by (7),

$$\sum_{\tau=t-T_g^{up}+1}^{t} u_g(\tau) \geqslant T_g^{up}\big(u_g(t-1) - u_g(t)\big), \tag{7a}$$

$$\sum_{\tau=t-T_g^{dn}+1}^{t} \big(1 - u_g(\tau)\big) \geqslant T_g^{dn}\big(u_g(t) - u_g(t-1)\big), \tag{7b}$$

where T_g^{dn} and T_g^{up}, respectively, represents minimum down and up time of unit g expressed as integer number of time steps. The rate at which a unit may increase or decrease generation is limited, therefore the generation level in one period is constrained by the generation level of the previous period plus the generation change achievable by the ramp rate over the amount of time in the period, as captured in (8),

$$p_g(t-1) - R_g^{dn}\Delta T \leqslant p_g(t) \leqslant p_g(t-1) + R_g^{up}\Delta T, \tag{8}$$

where R_g^{dn} and R_g^{up}, respectively, is ramp down and up rate of unit g.

- System constraints include power balance and reserve constraints. Power balance constraint ensures that the total power generation in each interconnected zone together with the power flow in/out, meet the zonal demand, as expressed in (9),

$$\sum_{g\in\mathcal{G}_i} p_g(t) + \sum_{l\in\mathcal{L}_i^{in}} f_l(t) - \sum_{l\in\mathcal{L}_i^{out}} f_l(t) = L_i(t), \tag{9}$$

where $\mathcal{G}_i$ denotes the set of generation units that belong to zone i, $\mathcal{L}_i^{in}$ and $\mathcal{L}_i^{out}$ respectively denote the set of paths with power flowing into and out of zone i, $L_i(t)$ is the load in zone i in period t, and $f_l(t)$ is the power flow of path l in period t, which must be within its power transfer capability, as expressed in (10),

$$-F_l(t) \leqslant f_l(t) \leqslant F_l(t). \tag{10}$$

In addition, system reserve constraint specifies reserve requirement such that the amount of generation capacity scheduled to be available can ensure the security of the operating system, as expressed in (11),

$$\sum_{g\in\mathcal{G}_i} r_g(t) \geqslant R_i(t) \tag{11}$$

where $R_i(t)$ is the system reserve requirement of zone i in period t, and $r_g(t)$ is the reserve provided by unit g in period t. The reserve from each unit g is limited by how much the unit can increase its power output from the scheduled base operating point, as expressed in (12),

$$p_g(t) + r_g(t) \leqslant u_g(t)\eta_g^{cap}(t)P_g^{max}. \tag{12}$$

3. Case study

The derating models of GT and CCGT together with the adapted UC formulation presented in previous section were implemented in Energy Operation Model (EOM), which was developed at Pacific Northwest National Laboratory to serve as an open source production cost tool for renewable integration studies. EOM repeatedly and automatically formulates UC as MILP problems and solves them by calling CPLEX through an evaluation period that can be customized. It outputs the production cost, generation by unit and category, fuel usage, locational marginal price (LMP), etc. The EOM model was previously validated against PROMOD, and in this paper we use EOM to quantify the heat wave impacts on EIC which is the largest electric grid in North America. The system configuration and generation dataset were obtained from the PROMOD IV NERC 9.0, in which the EIC model contains 4340 thermal generators in 39 interconnected zones, as given in Fig. 6. Please note that the five zones which include Canadian territory are excluded from this analysis.

In this study, we use the temperature during a normal summer period from weather stations in North American Land Data Assimilation System 2 from the National Aeronautics and Space Administration (NASA) [35] as baseline. To study the potential impacts of heat waves on the entire EIC, a heat wave with 10 °C uplifts is then constructed for all EIC zones for time period between 7/19/2006 and 7/24/2006. The default zonal load in the PROMOD database represents a regular year. The zonal load during a heat wave scenario is constructed using PROMOD zonal load and BEND model. In the BEND model, cumulated regional load changes during a heat wave are generated using EnergyPlus, a building level energy consumption model, together with a geospatial analysis of local environmental factors such as regional climate, population, building types, etc. Please refer [8] for details. As an example, Fig. 7 plots the temperature and load in American Electric Power (AEP) Zone for both baseline and heat wave scenarios. Compared with a normal summer day, the average load increases by 31% during the heat wave period.

3.1. Derating impacts on system reserve

The hourly generation capacity for GT and CCGT units is calculated using the temperature in both baseline and heat wave scenarios. For aggregated capacity of GT and CCGT, the hourly value in EOM and monthly value in PROMOD are compared in Fig. 8. As can be seen, in summer months from May to September, PROMOD underestimates the capacity by about 19 GW, which accounts for 9.0% of the total capacity from GT and CCGT. In winter months from October to April, PROMOD overestimates the capacity by about 3 GW.

Fig. 9 plots the nominal capacity and derated capacity of CCGT and GT in both normal summer days (7/15/2006–7/19/2006) and heat wave days (7/19/2006–7/24/2006). During normal summer

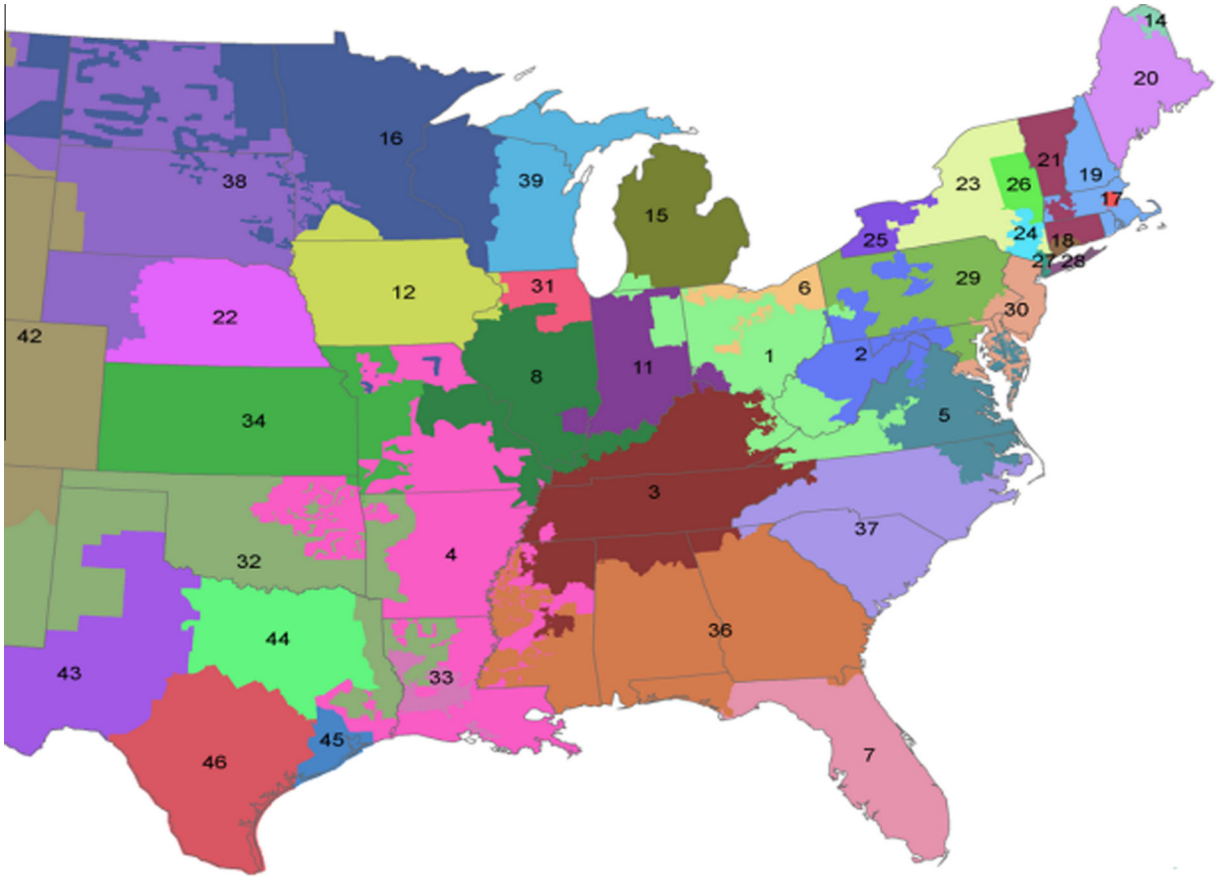

Fig. 6. Footprint of Eastern Interconnection including 39 zones.

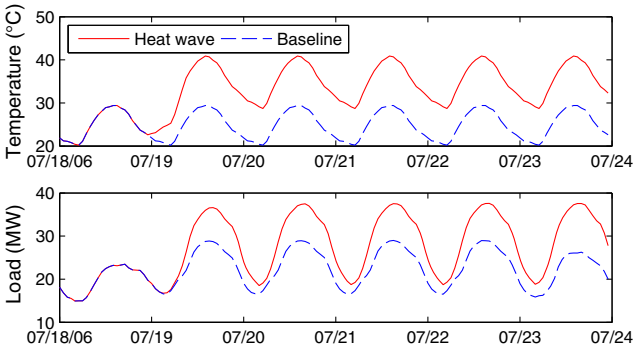

Fig. 7. Temperature and demand in AEP (zone 1) in baseline and heat wave scenarios from 7/18/2006 to 7/24/2006.

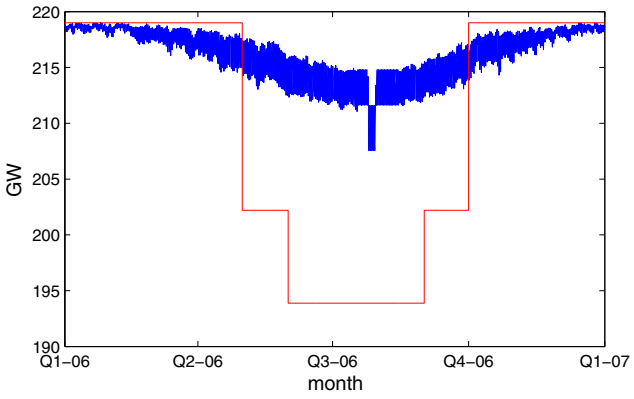

Fig. 8. Hourly derated capacity in EOM (blue) vs monthly capacity adjustment in PROMOD (red). (For interpretation of the references to color in this figure legend, the reader is referred to the web version of this article.)

days, the average actual capacity of CCGT and GT decreases 4.4 GW and 8.3 GW from its nominal value, respectively. During the heat wave period, the actual capacity can decrease as much as 5.5 GW and 10.2 GW for CCGT and GT, respectively. This accounts for 4.6% and 9.5% of their nominal capacities, respectively. The total capacity from CCGT and GT varies as much as 4 GW from day to night. Therefore, a fixed monthly derating factor cannot accurately represent varying capacity and estimate the corresponding system reserve and production cost.

During heat waves, the reduced capacity of CCGT and GT together with the increased cooling loads leads to a sharp drop in zonal reserve margin. The zonal reserve margin is the difference between the total capacity of committed units and peak demand, as percentage of the total zonal thermal capacity. In Fig. 10, the statistical attributes of zonal reserve margin for both normal summer days and heat wave days are provided in the form of a boxplot, where the circle in the box denotes the mean, the thick bar inside the box denotes the median, and bars outside the box denote first and third quartile. As can be seen, the reserve margin in heat wave days is significantly reduced in almost all the zones compared with normal summer days. In particular, there are only four zones with an average reserve margin less than 30% for normal summer days. This number increases to 14 zones for heat wave days. The average zonal reserve margin across EIC decrease 22.3% from normal days to heat wave days. For those zones with limited generation capac-

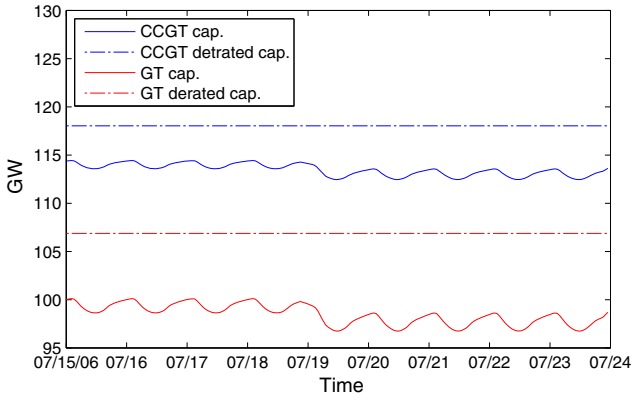

Fig. 9. Derated capacity of CCGT and GT units in EIC from 7/15/2006 to 7/24/2006.

ity, such as Zones 9, 15, and 21 (ISONEBOS, MINNESTA, NYZ-J), heat waves could lead to severe power shortage during peak hours.

3.2. Derating impacts on production cost

Four cases are developed to evaluate impacts of derating in capacity and efficiency on production cost and LMP, as listed in Table 1.

- Case 1 serves as a base case, where capacity of generators is modeled on a monthly basis, and heat rate is assumed to be constant regardless varying temperature. The study is performed using PROMOD.
- In Case 2, the capacity of GT and CCGT is modeled on an hourly basis using the ambient temperature, while the efficiency is modeled the same as Case 1.
- In Case 3, the efficiency of GT and CCGT is adjusted hourly based on ambient temperature, while the capacity is modeled the same as Case 1.
- In Case 4, derating effects in both capacity and efficiency are considered on an hourly basis. This case captures the heat wave impacts most accurately in production cost analysis.

Case 2 and 3 are first compared with Case 1 to quantify impacts of derating in capacity and efficiency separately. As an example, in Fig. 11, the LMP in ALWSTTA (zone 2) is plotted for heat wave days. The differences in LMP occur mainly in peak hours from 12 pm to 3 pm because (i) CCGT and GT are mainly used as peaking units because of their relatively high fuel cost compared with nuclear

Table 1
Case definition.

	Software	Capacity derating	Efficiency derating
Case 1	PROMOD	Monthly	Not considered
Case 2	EOM	Hourly	Not considered
Case 3	EOM	Monthly	Hourly
Case 4	EOM	Hourly	Hourly

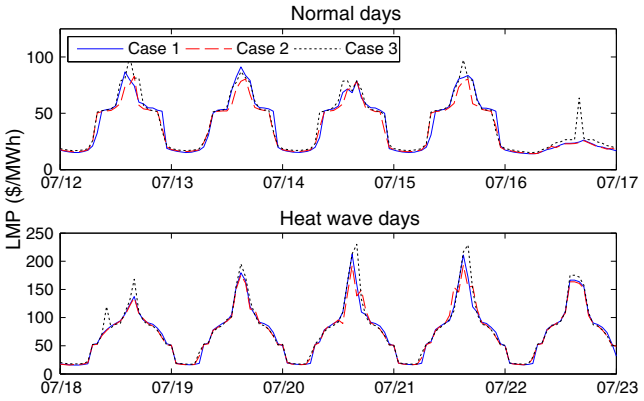

Fig. 11. LMPs in zone 2 ALWSTTA during 7/19/2006–7/24/2006.

and coal plants in 2006 in database NERC 9.0, and (ii) derating effects are most significant during these hours. The daily highest LMP in Case 1 is $9.6/MWh higher than Case 2 on average. This is because the monthly capacity in Case 1 underestimates the available capacity of CCGT and GT units during summer months. On the other hand, the daily highest LMP in Case 3 is $18.2/MW h higher than Case 1 because of the increased heat rate in Case 3. The average LMP in Case 1 is 0.6% higher than Case 2 and is 4.1% lower than Case 3.

The difference in production cost by generator category between Case 2 through 4 and Case 1 are plotted in Fig. 12, where "ST" represents "steam turbine". The following observation can be made.

- Case 2 has the lowest total production cost and production cost in CCGT and CT. This is consistent with the observation in LMP, as PROMOD underestimates the available capacity of CCGT and GT unit in summer months.
- Case 3 has the highest total production cost and production cost in CCGT and CT because (i) the monthly capacity consistently underestimates the varying available capacity, and (ii) the derated efficiency increases fuel usage.

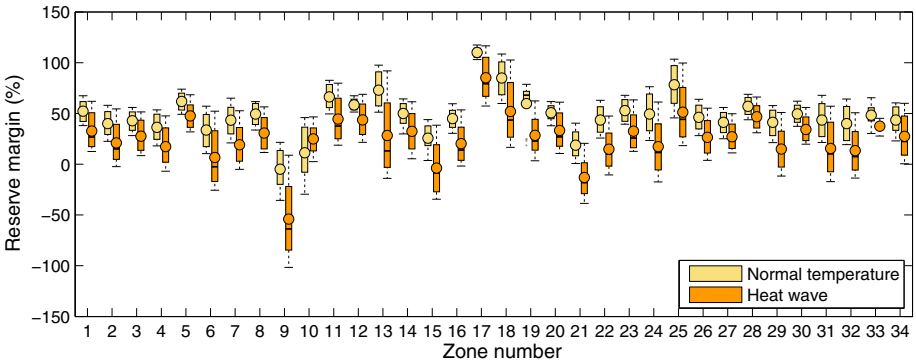

Fig. 10. Zonal reserve margin in regular summer days and heat wave days.

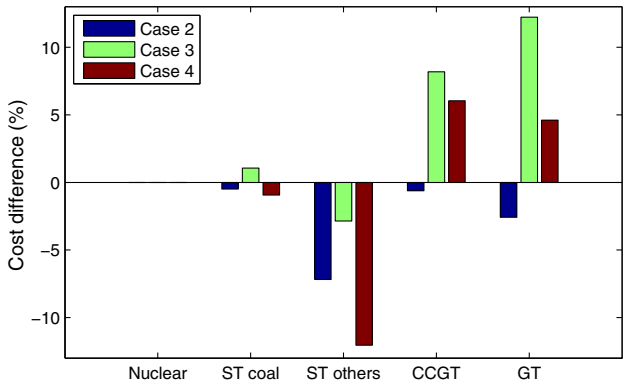

Fig. 12. Production costs in Case 2 through 4 compared with Case 1 by generator category.

- Case 4 represents the most realistic case, where hourly derating in both capacity and efficiency is captured. As expected, the total production cost and generation cost of CCGT and CT in Case 4 is higher than Case 2 but lower than Case 3 for aforementioned reasons.

In general, the degree to which the production costs are influenced by derating effects also depends on the fuel price of natural gas and the installed capacity of GT or CCGT. These are two key factors that determine the commitment results of GT and CCGT units. Because the cost of natural gas per BTU is higher than nuclear and coal in 2006 in NERC 9.0, the derating impacts are mainly limited to peak hours. Nevertheless, as natural gas price declines, generation cost of GT and CCGT becomes more cost-effective in serving the base load. In addition, as a result of economic, environmental, and technological changes in recent years, these gas-fired plants become increasing popular. According to Annual Energy Outlook 2015 by Energy Information Administration [29], the annual energy generated from natural gas plants has increased from 16% to 27% from 2000 to 2013, and they are expected to account for 31% of electricity generation by 2040. Therefore, the impacts of derating on system reserve and production cost are expected to further increase in the years to come.

4. Conclusions

This paper studies the potential impacts of heat waves on power grid operation. The derating effects capacity and efficiency of GT and CCGT are characterized as a function of ambient temperature. The UC formulation is then modified to incorporate the derating models. We have implemented the proposed method and evaluated heat waves impacts' for the EIC system. The results show that heat waves could significantly affect system reserve and production cost. Considering the derating impacts on an hourly basis is thus necessary to prevent: (1) underestimation of derating impacts in heat wave periods, which may cause severe power shortages and large price spikes, and (2) overestimation of derating impacts on the production cost in regular summer days, which may cause underuse of available generation capacity. Our future research will be focused on the co-optimization of thermal and water resources to address water availability and temperature impacts on generators in long-term planning.

References

[1] Zamuda C, Mignone B, Bilello D, Hallett KC, Lee C, Macknick J, et al. U.S. energy sector vulnerabilities to climate change and extreme weather. Tech rep DOE/PI-0013. U.S. Department of Energy; 2013.

[2] Meehl GA, Tebaldi C. More intense, more frequent, and longer lasting heat waves in the 21st century. Science 2004;305(5686):994–7. http://dx.doi.org/10.1126/science.1098704.

[3] Cook BI, Ault TR, Smerdon JE. Unprecedented 21st century drought risk in the American Southwest and Central Plains. Sci Adv 2015;1(1). http://dx.doi.org/10.1126/sciadv.1400082.

[4] Voisin N, Hamlet AF, Graham LP, Pierce DW, Barnett TP, Lettenmaier DP. The role of climate forecasts in western U.S. power planning. J Appl Meteorol Clim 2006;45(5):653–73. http://dx.doi.org/10.1175/JAM2361.1.

[5] Cohen SM, Averyt K, Macknick J, Meldrum J. Modeling climate-water impacts on electricity sector capacity expansion. In: ASME power conf. http://dx.doi.org/10.1115/POWER2014-32188.

[6] Lu N, Taylor T, Jiang W, Jin C, Correia J, Leung L, et al. Climate change impacts on residential and commercial loads in the western U.S. grid. IEEE Trans Power Syst 2010;25(1):480–8. http://dx.doi.org/10.1109/TPWRS.2009.2030387.

[7] Zhou Y, Clarke L, Eom J, Kyle P, Patel P, Kim SH, et al. Modeling the effect of climate change on U.S. state-level buildings energy demands in an integrated assessment framework. Appl Energy 2014;113:1077–88. http://dx.doi.org/10.1016/j.apenergy.2013.08.034.

[8] Dirks JA, Gorrissen WJ, Hathaway JH, Skorski DC, Scott MJ, Pulsipher TC, et al. Impacts of climate change on energy consumption and peak demand in buildings: a detailed regional approach. Energy 2015;79(1):20–32. http://dx.doi.org/10.1016/j.energy.2014.08.081.

[9] Kraucunas I, Clarke L, Dirks J, Hathaway J, Hejazi M, Hibbard K, et al. Investigating the nexus of climate, energy, water, and land at decision-relevant scales: the platform for regional integrated modeling and analysis (PRIMA). Climatic Change 2015;129(3–4):573–88. http://dx.doi.org/10.1007/s10584-014-1064-9.

[10] Wang J, Conejo AJ, Wang C, Yan J. Smart grids, renewable energy integration, and climate change mitigation–future electric energy systems. Appl Energy 2012;96:1–3. http://dx.doi.org/10.1016/j.apenergy.2012.03.014.

[11] Cohen SM, Rochelle GT, Webber ME. Optimizing post-combustion CO_2 capture in response to volatile electricity prices. Int J Greenhouse Gas Control 2012;8:180–95. http://dx.doi.org/10.1016/j.ijggc.2012.02.011.

[12] Wu D, Aliprantis DC. Modeling light-duty plug-in electric vehicles for national energy and transportation planning. Energy Policy 2013;63:419–32. http://dx.doi.org/10.1016/j.enpol.2013.07.132.

[13] de la Rue du Can S, Price L, Zwickel T. Understanding the full climate change impact of energy consumption and mitigation at the end-use level: a proposed methodology for allocating indirect carbon dioxide emissions. Appl Energy 2015;159:548–59. http://dx.doi.org/10.1016/j.apenergy.2015.08.055.

[14] Lu N, Wong PC, Leung LY, Scott M, Taylor T, Jiang W, et al. The impact of climate change on U.S. power grids. In: Proceedings of the second climate change technology conference, Hamilton, Ontario, Canada.

[15] Stewart WE. Turbine inlet air cooling. ASHRAE J 1998;40(9):32–7.

[16] Schewe PF. The grid: a journey through the heart of our electrified world. National Academies Press; 2007.

[17] Najjar YS. Efficient use of energy by utilizing gas turbine combined systems. Appl Therm Eng 2001;21(4):407–38. http://dx.doi.org/10.1016/S1359-4311(00)00033-8.

[18] ABB. PROMOD IV. <http://new.abb.com/enterprise-software/energy-portfolio-management/market-analysis/promod-iv>.

[19] Energy Exemplar. Plexos integrated energy model, <http://energyexemplar.com/software/plexos-desktop-edition/>.

[20] Carrión M, Arroyo JM. A computationally efficient mixed-integer linear formulation for the thermal unit commitment problem. IEEE Trans Power Syst 2006;21(3):1371–8. http://dx.doi.org/10.1109/TPWRS.2006.876672.

[21] Chen Y, Li J. Comparison of security constrained economic dispatch formulations to incorporate reliability standards on demand response resources into Midwest ISO co-optimized energy and ancillary service market. Electr Power Syst Res 2011;81(9):1786–95. http://dx.doi.org/10.1016/j.epsr.2011.04.009.

[22] Wang J, Wang J, Liu C, Ruiz JP. Stochastic unit commitment with sub-hourly dispatch constraints. Appl Energy 2013;105:418–22. http://dx.doi.org/10.1016/j.apenergy.2013.01.008.

[23] Zhao L, Zeng B, Buckley B. A stochastic unit commitment model with cooling systems. IEEE Trans Power Syst 2013;28(1):211–8. http://dx.doi.org/10.1109/TPWRS.2012.2196715.

[24] Ke X, Wu D, Lu N, Kintner-Meyer M. A modified priority list-based MILP method for solving large-scale unit commitment problems. In: Proc IEEE power energy soc gene meet. p. 1–5. http://dx.doi.org/10.1109/PESGM.2015.7286561.

[25] Valenzuela J, Mazumdar M, Kapoor A. Influence of temperature and load forecast uncertainty on estimates of power generation production costs. IEEE Trans Power Syst 2000;15(2):668–74.

[26] Geng Z, Chen Q, Chen X, Xia Q, Li J, Wang Y, et al. Unit commitment model including detailed modeling of combined cycle gas turbine concerning weather impacts. In: IEEE PowerTech, Eindhoven. p. 1–6.

[27] Guandalini G, Campanari S, Romano MC. Power-to-gas plants and gas turbines for improved wind energy dispatchability: energy and economic assessment. Appl Energy 2015;147:117–30. http://dx.doi.org/10.1016/j.apenergy.2015.02.055.

[28] Energy Information Administration. Electric power monthly; 2015. Available online at <http://www.eia.gov/electricity/monthly/epm_table_grapher.cfm?t=epmt_1_01>.

[29] Energy Information Administration. Annual energy outlook; April 2015. Available online at <http://www.eia.gov/forecasts/aeo/pdf/0383%282015%29.pdf>.
[30] Bloch HP, Soares C. Process plant machinery. 2nd ed. Elsevier; 1998.
[31] Dennis R et al. The gas turbine handbook. National Energy Technology Laboratory; 2006. Available online at <http://www.netl.doe.gov/research/coal/energy-systems/turbines/publications/handbook>.
[32] Viana A, Pedroso JP. A new MILP-based approach for unit commitment in power production planning. Int J Electr Power Energy Syst 2013;44 (1):997–1005. http://dx.doi.org/10.1016/j.ijepes.2012.08.046.
[33] Wood AJ, Wollenberg BF. Power generation, operation, and control. 2nd ed. John Wiley & Sons; 1996.
[34] Nowak MP, Römisch W. Stochastic Lagrangian relaxation applied to power scheduling in a hydro-thermal system under uncertainty. Ann Oper Res 2000;100(1):251–72. http://dx.doi.org/10.1023/A:1019248506301.
[35] National Aeronautics and Space Administration (NASA). North American land data assimilation system 2 (nldas-2). <http://ldas.gsfc.nasa.gov/nldas/NLDAS2model.php>.